NASA TECHNICAL MEMORANDUM

NASA TM X-71562

NASA TM X-71562

(NASA-TM-X-71562) GEOMETRY CONSIDERATIONS FOR JET NOISE SHIELDING WITH CTOL ENGINE-OVER-THE-WING CONCEPT (NASA) 40 p HC $3.25 CSCL 01C

N74-25568

Unclas G3/02 40698

GEOMETRY CONSIDERATIONS FOR JET NOISE SHIELDING WITH CTOL ENGINE-OVER-THE-WING CONCEPT

by U. von Glahn, D. Groesbeck, and M. Reshotko
Lewis Research Center
Cleveland, Ohio

TECHNICAL PAPER proposed for presentation at
Seventh Fluid and Plasma Dynamics Conference
sponsored by American Institute of Aeronautics
and Astronautics
Palo Alto, California, June 17-19, 1974

ABSTRACT

Jet noise shielding benefits for CTOL engine-over-the-wing installations were obtained with various model-scale circular nozzles and wing chord geometries. Chord-to-nozzle diameter ratios were varied from 3 to 20, while ratios of nozzle height above the wing to the diameter were varied from near zero to 3. Spectral noise data were obtained with jet velocities from 640 to 1110 ft/sec. Characteristics of low frequency noise sources are discussed. Jet-noise shielding is correlated in terms of acoustic and geometric parameters. Implications of extending the model-scale data to full-scale are discussed.

E-7991

GEOMETRY CONSIDERATIONS FOR JET NOISE SHIELDING WITH CTOL ENGINE-OVER-THE-WING CONCEPT

by U. von Glahn[1], D. Groesbeck[2], and M. Reshotko[3]

V/STOL and Noise Division
Lewis Research Center
National Aeronautics and Space Administration
Cleveland, Ohio

E-7991

INTRODUCTION

In order to help meet acceptable community noise standards for future conventional takeoff and landing (CTOL) aircraft, the engine exhaust nozzle can be placed over the wing (OTW) as shown schematically in figure 1. With such an engine-airframe configuration, the ground observer is shielded by the wing from much of the engine exhaust noise radiated to the ground.

With a CTOL-OTW configuration the most prominent noise sources, as indicated in figure 2 appear to be the engine exhaust jet noise, engine core noise, scrubbing noise produced by the exhaust flow over the wing surface, and trailing edge noise caused by an interaction between the edge and the jet flow. Because the jet exhaust flow for a CTOL application is not required to be attached to the wing surface, as in the case for powered-lift OTW configurations, it should be possible to minimize the scrubbing and trailing edge noise by locating the nozzle exhaust well above the wing surface so that the flow is negligibly attached to the surface. However, an acoustic impedance between the trailing edge and the nozzle flow field is still a possible noise source although the jet flow is completely unattached.

Jet-noise shielding accomplished by a wing is similar to that observed on the ground by the erection of a barrier between a noise source and an observer. The main differences between the two applications of "barrier shielding" are the nature and generation mechanisms of the noise source and the close proximity of the noise source to the shielding surface for aircraft compared with ground barrier applications. With respect to the noise source, the distributed noise generation obtained with a jet near the surface increases the analysis complexity as compared with a "point" noise source normally assumed for ground applications.

---

[1]Member AIAA, Chief, Jet Acoustics Branch.

[2]Aerospace Research Engineer.

[3]Member AIAA, Aerospace Research Engineer.

The noise shielding capability of a wing for the CTOL engine-over-the-wing concept has been studied experimentally with several small-scale models (refs. 1 to 3) and to a more limited extent with a large-scale configuration (ref. 4). A typical example of jet noise shielding by a wing is shown in figure 3, wherein the sound pressure level is plotted as a function of frequency for the cases of nozzle alone and nozzle with wing. The addition of the wing causes an increase in low frequency noise and a decrease in high frequency noise (shielding). The amount of low frequency noise amplification, on the basis of limited data, appears to depend on shielding surface (wing) length, location of the nozzle with respect to the surface, nozzle diameter, jet velocity, relative velocity (forward speed effects) and distance from the trailing edge of the wing to the unattached jet flow. Of particular significance to aircraft application of the concept is the fact an increase in the model scale appears to reduce the low frequency noise amplification. Thus, the published small-scale acoustic data appear to yield pessimistic, i.e. high, SPL values when projected to full scale.

On the basis of the references cited previously, the acoustic shielding benefits derivable from wing shielding of jet noise appear to be functions of shielding surface length, nozzle diameter, jet velocity, relative velocity and flap deflection.

The present study conducted at the NASA Lewis Research Center was directed toward establishing the effect of nozzle location and wing size, relative to the nozzle size, on the acoustic characteristics, including jet noise shielding and low frequency noise sources, of model OTW configurations using a conical nozzle. In addition, the forward velocity effect on noise directivity and spectra was evaluated for a selected OTW configuration. Acoustic data are presented using convergent circular nozzles ranging from 1.1 inches to 13 inches in diameter. The "wings" used consisted of airfoil sections as well as simple boards and ranged from 8.5 inches to 82 inches in chord length depending on the specific nozzle size. The height of the nozzles above the wing was varied from height-to-nozzle diameter ratios of near zero to 2.75. Most of the noise data are for a "retracted flap" geometry; however, some data for "flap deflected" cases are also shown.

Acoustic results are presented in terms of spectral data. The data were obtained over a range of nominal jet exhaust velocities from 640 to 1110 ft/sec and forward velocities of 0 and 175 ft/sec. Tentative correlations of acoustic shielding benefits and jet-surface interaction noise are presented. On the basis of the correlation parameters developed, small-scale model spectral shielding data are compared briefly with unpublished shielding data obtained with NASA Quiet Engine C.

APPARATUS AND PROCEDURE

Facilities

The acoustic data used herein were obtained from tests conducted primarily at three test sites. Small-scale model data with a nominal 2-inch diameter nozzle and 13-inch chord wing were obtained using the free-jet facility described in reference 1. Large-scale model data were obtained using a 13-inch diameter nozzle and 7-foot chord wing in the cold-flow facility described in reference 4. The major portion of the present work was obtained at a site situated within the courtyard area of a large subsonic wind tunnel and described in reference 5. Finally, unpublished preliminary data obtained at the Lewis Research Center with a full scale engine (NASA Quiet Engine C, ref. 6) and a large wing are compared with data obtained using a bypass nozzle at the small-scale model site (ref. 1).

Because the nozzle-surface geometry effects on shielding were made primarily with the courtyard rig, a brief description of this rig is included herein for convenience.

E-7691

A schematic sketch of this facility is shown in figure 4. Pressurized air at about 530° R was supplied to a 6-inch diameter plenum by twin diametrically opposed supply lines. Airflow through the overhead supply line was measured with a calibrated orifice. The nozzle inlet total pressure was measured with a single probe near the plenum exit flange. Pressure data were recorded from suitable multitube manometers. Perforated plates and a muffler were located in each system to remove valve noise from the measured noise. In addition, a bundle of tubes was placed in the plenum to straighten the air flow before it reached the entrance to the nozzle. These devices were located well upstream of the nozzle. Open-cell foam pads were used in an effort to minimize reflections from the surrounding walls. In addition, foam pads were also placed on the ground to determine the importance of ground reflections on the acoustic data.

Sound pressure level (SPL) spectra were obtained using a 0.5-inch diameter condenser microphone with wind screen. Data were recorded at 90° to the jet axis at a 10-foot radius. The noise data were recorded on a FM tape recorder and digitized by a four second time averaged one-third octave band spectrum analyzer. The analyzer determined sound pressure level spectra in decibels referenced to 2×10^{-5} N/m^2.

Test Models

The nozzles used at this test site consisted of simple tubing reducers resulting in exhaust diameters of 1.1 and 2.1-inches. For the

most part, simple boards (1/2-inch thick plywood) of 24-inch span and surface lengths downstream of the exhaust nozzle of 5.9, 10.4 and 21.4 inches were used (fig. 5). The usual surface length upstream of the nozzle exhaust plane was 2.6 inches; however, lengths up to 13.6 inches were also studied. Finally, the 13-inch wing used in previous studies (ref. 1) was also tested with the 2.1-inch diameter nozzle to provide a comparison of the acoustic measurements from the present test site and that used in previous work. Acoustic data taken at this site were obtained at nominal jet velocities from 640 to 1110 ft/sec.

Jet velocity profiles were obtained at the downstream trailing edge of the various shielding surfaces used at the small-scale flow rig. Measurements were made with a traversing pitot static tube. The pressures measured were transmitted to an x-y-y' plotter which yielded direct traces on graph paper of the total and static pressure distribution across the jet. All other pressures were recorded from mercury and water manometer boards.

Sketches of the various configurations used in references 1 and 4 and the full-scale engine studies are shown in figures 6 to 8, respectively.

GENERAL CONSIDERATIONS

Aerodynamic

Velocity profiles were taken at the downstream end of the shielding surface for all 1.1- and 2.1-inch diameter nozzle-board configurations. The profiles, shown in figure 9, are on the nozzle centerline at right angles to the board and were obtained from cross-plots of surveys taken parallel to the board. These data shown in figure 9 are in terms of local Mach number and radial height above the surface. The effect of the nozzle height above the surface on the velocity profile is negligible except when the nozzle is near the surface. When the nozzle is located close to the shielding surface and/or the surface length is large, the jet plume scrubs the surface. The scrubbing velocity increases with decreasing height of the nozzle above the surface and increasing surface length.

With a long shielding surface, the jet velocity at the trailing edge is reduced by the normal jet decay process compared to that associated with short shielding lengths. The peak velocity at the trailing edge of the long shielding surface again is not altered by the proximity of the nozzle to the surface.

Acoustic Characteristics of Courtyard Rig

The test site of reference 5 can be classed as a non-acoustic arena because of the presence of the wind tunnel walls enclosing the test site. However, studies have shown that parametric variations in acoustic measurements can be obtained when properly normalized to data taken in an acoustic arena such as the test site of reference 1. In general, the spectral data on a broadband basis in the courtyard test site are slightly higher with the 2.1-inch diameter nozzle, with and without a wing, than that taken in the arena of reference 1. Although the nozzle contraction contours for the nozzles used at the two sites differed as well as the airflow muffling systems, the difference in SPL level is attributed mainly to the arena itself. Comparisons of the SPL spectra for similar jet velocities are shown in figure 10 using the 13-inch chord wing at both test sites and normalized to the same nozzle SPL level. Good agreement is achieved between spectral data taken at the two sites. (The differences in SPL for configurations with and without a wing were not influenced by the site location as is apparent from figure 10.) Analysis of the 1.1-inch diameter nozzle-only data indicated that the broadband reduction in SPL level required to correlate the data with that taken in a good acoustic arena was less than 1 dB.

All the data taken at the courtyard site have been normalized for the effects just discussed.

E-7991

Comparison of Data Taken With Board and Wing

The acoustic data taken with a flat surface (board) differs somewhat from that taken with an airfoil surface. With an airfoil (ref. 1), because of the upper surface wing curvature, the trailing edge is farther away from the centerline and boundary of the jet than in the case of a flat surface even though the nozzle heights at the nozzle exhaust plane are identical. An example of the effect of this increase in height at the trailing edge of the surface on the SPL spectra is shown in figure 11. The data shown are for the 2.1-inch nozzle located 0.57 inches above the respective surfaces (board and wing) at the nozzle exhaust plane. The local SPL values in the range of 1000 to 3150 hertz are up to 5 dB higher with the board than with the wing.

When the board was pivoted at the nozzle exhaust plane (see fig. 5) by an angle α, the noise level in the low and middle frequencies was significantly reduced. An example of such data is shown in figure 12 wherein the board, located 1.25 inches below the nozzle lip (2.1-inch diameter nozzle), was pivoted over a range of angles from 0 to 15°. Increasing the distance of the board trailing edge away from the nozzle centerline caused a general decrease in interaction noise in the 200 to 2000 hertz range.

Comparison of the available acoustic data shown in figures 10 and 12 indicates that an effective height of the nozzle above the surface, h_e, defined by $h + h_{te}/2$ where h_{te} is the difference in height between the surface at the exhaust nozzle plane and the trailing edge, both referenced to the nozzle axis, gives a good estimation of the effect of wing thickness on jet-surface interaction noise level.

It is also apparent from the data in figure 11 that jet noise shielding benefits (frequencies generally above 2000 hertz) are the same with the board and the wing. Furthermore, a change in board angle (fig. 12) has no apparent effect on the shielding of jet noise over the range of variables noted for the data shown.

NOISE SOURCES

A cursory examination of the spectral data of figures 10 to 12 appears to indicate two noise sources; one near 500 hertz and the other near 1500 hertz. A study of SPL spectra over the wide range of geometry variations included in this study indicates that the noise sources consist of what can be classed as broadband edge tones or haystacks. These haystacks penetrate above the nozzle spectral noise level and become the dominant low frequency noise sources.

In the present work, two major haystack noise sources were identified. These sources, designated by Roman numerals I and II, are shown in figure 13 for a 1.1-inch diameter nozzle with a 10.4-inch shielding surface with the nozzle height 0.57 inches above the surface. In the particular case shown, the haystack noise sources appeared to peak near 500 and 1500 hertz. The noise sources individually varied with nozzle height above the surface, length of shielding surface, jet velocity and forward velocity. It is these variations in the spectra that lead to the noise source representation shown in figure 13. Presently, noise source I is believed to be caused by trailing edge interactions with the jet flow while noise source II, which disappears rapidly with increasing nozzle height above the surface, is believed to be related to scrubbing noise of the jet flow on the surface. Trends in the number and noise level of these haystacks, as related to nozzle-surface geometry variations and flow conditions, are discussed in the following sections.

Factors Affecting Noise Sources

Effect of nozzle height above surface.- Increasing the nozzle height above the shielding surface generally caused the SPL level to become less for all the noise sources. This trend is shown by the SPL spectral plot in figure 14 for the 1.1-inch nozzle with a shielding surface length, L, of 10.4 inches and a jet velocity of 640 ft/sec. Noise

source II in figure 14 influences the initiation of shielding (circle symbols compared with other symbols); however, at high frequencies the shielding is substantially independent of the low frequency noise sources. Similar data trends were noted for the 2.1-inch diameter nozzle.

Effect of surface shielding length on noise sources.- The effect of an increase in shielding surface length on the level and characteristics of the noise sources is shown in figure 15. The data shown were obtained with the 1.1-inch nozzle located 0.57-inches above the surface and at a jet velocity of 640 ft/sec. The data shown are for shielding surface lengths of 5.9 and 21.4 inches, and an L_f of 2.6 inches. Increasing the surface length caused a reduction in SPL level of noise source II and caused this noise source to be dominated by the jet noise level. However, noise source I was substantially increased by using a longer shielding surface. The peak frequency for each noise source was decreased by increasing the surface length. With an increase in the height of the nozzle above the wing (to 3 inches) and a short shielding surface (5.9-inches) only noise source I was identifiable; the other sources being dominated by the jet noise spectrum.

The variation of L_f given in figure 5 did not significantly affect the sound pressure level spectra for the configurations tested. Consequently, the data shown herein are primarily those for an L_f of 2.6 inches.

The data also show that the jet noise shielding is improved in terms of a reduction in SPL at a particular frequency as well as the extent of the frequencies over which the shielding benefits occur by an increase in shielding length. Similar trends were obtained with other nozzle heights above the shielding surface and nozzle diameters.

Effect of jet velocity.- The effect of jet velocity on the noise sources is shown in figure 17 for the 2.0-inch nozzle and 13-inch chord wing partially reported on in reference 1. The data shown are for a nozzle height of 0.44-inches above the wing, a jet velocity of 840 ft/sec and forward velocities of 0 and 175 ft/sec. Because of the limited low frequency range available with the free jet tests, only noise source II is readily apparent with only a portion of noise source I being identified. Also shown for comparison are the spectral data for the nozzle operating in the free jet without a wing (ref. 7). A comparison of the noise source levels in figure 17(a) shows that forward velocity reduces the peak SPL values of the sources; however, the SPL reductions achieved appear to be different functions of the relative velocity, $U_j - U_o$. The SPL level for noise source I appears to follow a 7 to 8 exponent of the relative velocity while noise source II appears to follow a 5 exponent. With the nozzle located 1.75 inches above the wing, the data of reference 1 indicates only noise source I dominates jet noise and follows a 7 to 8 exponent of the relative velocity. The nozzle only data shown in figure 17(b) follows a 6-exponent of the relative velocity (ref. 7).

Directivity aspects of noise sources.- The effect of directivity or radiation angle on the SPL level of the noise sources is illustrated in figure 18 for the 2-inch conical nozzle with 13-inch chord wing of reference 1. The data are for a jet velocity of 840 ft/sec with the nozzle 0.44-inch above the wing and without forward velocity and with a forward velocity of 175 ft/sec. Without forward velocity noise source I shows that substantially the same SPL level is obtained for all directivity angles from 60° to 120°. Noise source II indicates a small effect of directivity angle, with the SPL levels increasing somewhat as the directivity angle increases from 60° to 120°. The frequency associated with the peak SPL value for each noise source appears to be independent of directivity angle. In comparison, for the same directivity angles the change in the peak SPL level for the nozzle-only amounted to twice those shown in figure 18. Substantially similar trends with directivity angles were determined for the noise sources with forward velocity as shown in figure 18.

Large-Scale Model Data

Extrapolation of the small-scale data indicates that with increasing model size and jet velocity, jet-wing interaction noise will become less of a dominant noise source for full scale CTOL-OTW commercial aircraft. Comparison of data taken with the large-scale model of reference 4 (13-inch diameter nozzle and 84-inch chord) with that from the present work substantiate this observation. Jet-wing interaction noise source I peaked near 160 hertz and resulted in an apparent local increase in SPL level of less than 3 dB with jet velocity of 670 ft/sec (ref. 4). Noise source II could not be detected. Even less interaction noise was observed at a jet velocity of 940 ft/sec (ref. 4).

Correlation of Noise Sources

The peak SPL value for both of the jet-surface interaction noise sources and the associated frequencies were empirically correlated by the following relationships that were developed on the basis of the parametric small-scale model experimental data. The correlation was made in order to facilitate interpretation of small-scale model data and its extrapolation to large scale.

The frequency at which each peak SPL occurred can be approximated by the following equation:

$$f_p = \frac{f_b}{\left(1 + 0.025\,\frac{L}{D}\right)\left[1 + \left(\frac{B\,gh}{a_o^2}\right)^4\right]}, \text{ Hz} \qquad (1)$$

where

(1) for noise source I, f_b = 550 hertz and B = 10^5

and

(2) for noise source II, f_b = 1650 hertz and B = 2×10^5.

The SPL level for each noise source with zero forward velocity is correlated by the following relationship:

$$SPL^* \sim \frac{f_p L}{a_o} \tag{2}$$

where

$$SPL^* = SPL_p + 10 \log \left[1 + \left(\frac{h}{D} \right)^2 \right]$$

$$- 10 \log \left(\frac{\rho_o U_j^m D^2}{a_o^{m-3}} \right) - 10 \log \left(\frac{f_b a_o \times 10^{-4}}{g} \right) \tag{3}$$

The jet velocity exponent, m, is taken as 3 for noise source I and 6 for noise source II.

The peak sound pressure level values, SPL_p, of noise sources I and II are shown correlated by use of equations (1) to (3) in figure 19. Reasonable correlation on the basis of limited data is evident. The correlation was developed for data taken at a directivity angle of 90°. However, as indicated in figure 18, the effect of directivity angle is small and is assumed negligible for gross-order calculations over the range of directivity angles of interest (60° to 120°).

The effect of forward velocity can be included by adjusting the SPL levels of the noise sources, including the nozzle-only level by use of the relative velocity and the appropriate exponent for relative velocity, $U_j - U_o$, discussed earlier. At the present time, relative velocity exponents, n, of 7.5 and 5 are recommended for noise sources I and II respectively. An n-exponent of 6 applies to nozzle-only spectra (ref. 7).

The spectral distribution for the noise sources can be determined from figure 20 in which the difference between the peak SPL and the local SPL values is shown as a function of 1/3-octave band frequencies. The spectral plot for noise source I appears to be somewhat narrower than those for noise source II. Noise source I appears to approach a fall-off rate of about 6 dB/1/3-octave at frequencies below the peak frequency and 5 dB/1/3-octave at frequencies greater than the peak frequency. Noise source II shows values of 5 and 4 respectively for the same situation.

The use of the noise source correlation given by equations (1) to (3) and the plots in figures 19 and 20 for acoustic predictions will be discussed in a later section.

JET NOISE REDUCTION BY SURFACE SHIELDING

The shielding of jet noise by an airframe component such as a wing is related to that commonly encountered in shielding noise sources on the ground by erecting barriers such as solid fences or walls. It could be assumed, therefore, that existing barrier shielding theory can be used to estimate the shielding of jet noise by a wing. Subtle differences exist, however, that make this difficult.

Noise shielding by a barrier on the ground considers the acoustic source to occur substantially at a point. Furthermore the noise attenuation is a function of relatively large distances for both the source and the observer from the barrier. A typical relationship is shown in figure 21 taken from reference 8. Although theory indicates no limit to shielding, practice indicates there may be an effective limit in the order of 25 dB at very high frequencies (ref. 9).

For a CTOL-OTW aircraft, the exhaust jet is located relatively close to the wing surface and is a distributed noise source. The noise obtained at the various frequencies of such an acoustic source, is therefore generated at different distances from the surface and at different locations relative to the edge of the barrier (wing or flap trailing edge). An analytical model of the jet noise-source distribution, therefore, would have to include a complex integration to sum up the contributions of all the jet noise sources with their local surface shielding lengths.

The present approach employs empirical correlations of existing data to arrive at a prediction method for the shielding of jet noise by a wing-flap system. The analysis leading to the data correlation is given in terms of the SPL difference between nozzle-plus-shielding-surface and the nozzle-only, $SPL-SPL_N$ or ΔSPL.

A typical plot of ΔSPL as a function of frequency for a CTOL-OTW configuration is shown in figure 22. Positive ΔSPL values indicate that jet-surface interaction noise sources are dominant over the nozzle-alone jet noise while negative ΔSPL values indicate jet noise shielding by the wing-flap system. Four basic noise regions, denoted by A, B, C, and D are indicated in figure 22. Region A is characterized by noise amplification over that caused by nozzle-alone jet noise and is attributed to jet-surface interaction noise sources. Region B is a transition region into the shielding regime that is a function of the interplay between the regions of interaction noise sources and jet noise shielding. When the interaction jet-surface noise sources are strong (large positive ΔSPL values) the slope of this transition region is steep; whereas when they are weak, the slope of this transition region is shallow and blends rapidly into the jet noise shielding portion of the curve shown. Region C typifies a "barrier" shielding curve. The region C data are used herein to correlate jet noise shielding ΔSPL values. Region D frequently shows a reduced jet noise shielding capability at high frequencies inconsistent with barrier shielding analyses. The exact reasons for reduced jet noise shielding are not understood; however, it is believed that the reduced attenuation is primarily an aero-acoustic interaction anomaly associated with a specific nozzle-wing configuration and reflects the presence of a high frequency noise floor. For jet noise shielding correlation purposes, the data in regions B and D will not be used in order to avoid the obvious data ambiguities.

The following sections discuss the various nozzle-wing system geometry effects on jet noise shielding and present data and correlation procedures by use of empirically determined parameters and equations. Except as noted the data are for a directivity angle of 90° and a nominal jet velocity of 670 ft/sec. It should be noted that the solid curves shown in figures 23 to 28 are calculated from correlation equations to be discussed later and are not faired curves through the data points.

Effect of surface length.- With increasing surface length the ΔSPL at a given frequency is increased. The effect of surface length is shown correlated in figure 23 in terms of ΔSPL as a function of the product of frequency and surface length fL, for region C data and at a nozzle height, h, of 3 inches. The data shown are for a 2.1-inch diameter nozzle and an L_f of 2.6 inches. Good correlation of the noise data on the basis of surface length is apparent as would be expected from barrier theory. It should be noted that variations in L_f over the range indicated in figure 5 did not affect ΔSPL shielding values, consequently the L_f values in the following sections are not identified.

Zero Flap Deflection

Effect of nozzle height above surface on shielding.- On the basis of the present tests, the height of a conical nozzle above the shielding surface does not appear to have a significant effect on noise attenuation caused by the shield. While this statement appears to be at variance with barrier noise attenuation theory, it applies to the aircraft case because engine exhaust nozzles for OTW applications generally would be within a diameter or two of the wing surface due to structural and weight considerations. Consequently, at directivity angles of interest for aircraft the shadow angle ϕ (fig. 21) would not significantly change with nozzle height.

The amount of shielding, in terms of ΔSPL as a function of frequency, is shown in figure 24 for several nozzle heights above the surface. The data are for a 2.1-inch diameter nozzle and a shielding surface length of 10.4 inches. The data contained within region C are noted. It is apparent that at the higher frequencies the amount of shielding obtained is substantially independent of the nozzle height above the surface. The initiation of jet noise shielding, however, is a function of nozzle height. With increasing nozzle height above the surface the shielding benefits begin at correspondingly lower frequencies. The initiation of shielding is tied to the noise sources discussed previously and can be estimated by a method of superposition to be discussed later.

Effect of nozzle diameter on shielding.- On the basis of the preceding sections, the effects of surface length and jet velocity on the shielding of jet noise can be shown to be a function of a Strouhal relationship given by fL/U_j. However, an additional variable, namely, the nozzle size also affects jet noise shielding. Analysis of the available data over the range of nozzle diameters from 1.1 to 13 inches showed that the effect of nozzle size could be expressed by a dimensionless term as follows:

$$\left(\frac{a_o^2}{gD}\right)\left[1 + 4.5\times10^9 \left(\frac{gD}{a_o^2}\right)^2\right] \tag{4}$$

By combining the Strouhal relationship, fL/U_j, with equation (5), the following jet noise shielding parameter evolves:

$$\Delta SPL \sim \left(\frac{fLa_o^2}{gDU_j\times10^6}\right)\left[1 + 4.5\times10^9 \left(\frac{gD}{a_o^2}\right)^2\right] = Q \tag{5}$$

Shielding data for region C plotted in terms of the parameters of equation (5) are shown in figure 26. The data are for nozzle diameters of 1.1, 2.1 and 13 inches with surface lengths, L, of 5.9, 10.4 and 69 inches, respectively. It is apparent that good data correlation on the basis of the relationship given by equation (5) has been achieved.

Directivity effects on shielding.- For directivity angles differing from 90°, the ΔSPL can be expected generally to decrease since the effective surface shielding length (view factor) is decreased although the value of ϕ may increase and offset this trend in the view factor. In general, the data substantiate this; however, in some instances, notably at a θ of 140°, greater negative ΔSPL values than expected were obtained when the nozzle was nearly on the shielding surface. With the exception of such anomalies, the data for the directivity angles of interest (60° - 120°) was correlated reasonably well by the inclusion of a simple directivity parameter as follows:

$$\Delta SPL \sim \left[\frac{1}{1 + 0.033\left(\frac{\theta}{180 - \theta}\right)^4}\right] Q = Z \qquad (6)$$

Typical examples of data correlation for various directivity angles are shown in figure 27 for data reported in references 1 and 4. For a more precise representation of the directivity effect on shielding, more extensive analyses, well beyond the scope of the present work, will have to be employed.

Effect of forward velocity.- The effect of forward velocity on jet noise was reported in reference 7. The results of this study showed that, considering the limited scope of the tests, the majority of the sound pressure level with forward velocity could be correlated in terms of a Strouhal relationship as a function of jet velocity rather than relative velocity. It should be noted, however, that the forward velocity effect lengthens the core of the jet exhaust compared with its length for static conditions. This could alter the jet noise source distribution although the effect may be small. When a wing or shield is added, any alteration of the jet noise sources by forward velocity could change the jet noise shielding effectiveness compared with static conditions. While some data do indicate a small reduction in shielding effectiveness with forward velocity an equal amount of data indicates no change or a small increase (ref. 1). Because of this uncertainty in the available data, the acoustic data presented herein with forward velocity is correlated in terms of the jet exhaust velocity (eqs. (5) and (6)) rather than as a function of relative velocity.

Typical data taken from reference 1 and illustrating the effect of forward velocity on jet noise shielding are shown in figure 28. The data

are for a 2-inch diameter conical nozzle located 0.44 inches from the surface of a 13-inch chord wing (L, 10.4-in.). The data are for a jet velocity of 940 ft/sec and forward velocities of 0 and 175 ft/sec. The ΔSPL values for the static and forward velocity data are substantially identical. This means that absolute values of jet noise shielding are reduced by forward velocity in the same manner as jet velocity; namely by the 6-power of the relative velocity, $(U_j - U_o)^6$.

Jet Noise Shielding Correlation

As stated in the introduction to this section only region C in figure 22 was used for correlation of jet noise shielding because regions B and D are considered to be configuration oriented phenomena. An equation that fits the data shown in the previous figures can be written as follows for static conditions:

$$\Delta SPL = 10 \log (1 + 0.6Z) \qquad (7)$$

The solid curves shown previously in figures 23 to 28 were generated by use of equation (7).

Shielding with Flaps Deflected

The work reported in references 2 to 4, included tests made with and without flaps deflected. With flaps deflected it would be expected, on the basis of the effects of board angularity changes shown in figure 12, that the jet-surface interaction noise would be reduced while the jet noise shielding would be substantially the same. The latter, however, is true only if the projected or effective shielding-surface length is not increased by the extension of the flap system. Furthermore, open slots between the wing and flap components could permit noise to escape toward a ground observer.

The small-scale model data of references 2 and 3 used only a covered flap system while the large-scale model data of reference 4 evaluated both covered and open-slot flap systems.

The effect of flap deflection on shielding effectiveness is shown in figure 29 for the large scale model of reference 4 with flap slots closed in terms of ΔSPL as a function of the correlation parameter Z. The L-term in the Z-parameter is the projected length of the wing-flap system downstream of the nozzle exhaust plane and parallel to the nozzle axis. It is apparent that deflection of the flaps to either 20° or 60° increases the overall jet noise shielding by an equal amount of about 2.5 dB in region C. With the flap slots open, shielding was decreased

by up to 2 dB over the entire jet noise frequencies subject to shielding compared to closed-slot flaps. Although not shown, no significant changes in the noise source at low frequencies were observed between the slots open and closed configuration.

Similar acoustic data taken with the small-scale model of reference 2 and 3 did not appear to indicate the deflected flap trends evident in the large-scale model data.

Correlation of the large-scale model data with flaps deflected can be obtained by the following equation which is a modification of equation (7):

Flap slots closed

$$\Delta SPL = 10 \log (1 + 1.4Z^{0.85}) \tag{8}$$

Flap slots open

$$\Delta SPL = 10 \log (1 + Z^{0.925}) \tag{9}$$

These equations represent a best fit curve to the large-scale model data of reference 4. The dashed curve in figure 29 was generated by use of equation (8).

Comparison of Small-Scale Model Data with Engine Data

Unpublished data obtained at NASA-Lewis with Quiet Engine C in a CTOL-OTW configuration (fig. 8) is shown in figure 30 compared with data obtained using a small-scale model (fig. 6(b)). While the configurations differed somewhat, both used bypass-type exhaust nozzles. The small-scale model nozzle-wing configuration is that reported in reference 1. The engine-nozzle configuration is described in reference 6. The exhaust nozzle plane of the fan flow was located at the leading edge of a simulated wing resulting in a shielding length of about 14-ft downstream of the core nozzle. For the small-scale bypass nozzle the core exhaust was located at the 20 percent chord point. The core jet velocities were 840 and 1190 ft/sec for the small-scale model and engine, respectively. A comparison of the jet noise shielding at a directivity angle of 100° obtained with these configurations indicates reasonable correlation in terms of the Z-parameter as shown in figure 30. Above 12,500 hertz (not shown in figure), the ΔSPL values for the engine data decrease with increasing frequencies. In general, the cold-flow, small-scale model shielding data correlate well with full-scale engine shielding data. It should be noted that the full-

scale engine data indicated that jet noise dominated the interaction noise sources since no significant positive values of ΔSPL were obtained over the entire frequency spectrum from about 63 to 20,000 hertz.

PREDICTION OF ACOUSTIC SPECTRA FOR CTOL-OTW CONFIGURATIONS

On the basis of the empirical correlations developed for both the additional low frequency noise and the jet noise shielding, a method of superposition is proposed by which the spectral noise distribution can be predicted for unattached-flow CTOL-OTW configurations. An outline of this method of superposition follows together with schematic sketches illustrating the procedure.

The following steps are proposed in developing the spectrum at any directivity angle:

1. Plot the nozzle-alone spectrum in terms of sound pressure level as a function of frequency (fig. 31(a)).

2. The absolute value of SPL_p is then obtained for each noise source from equation (3) for which SPL^* is determined at the desired shielding length, L, from figure 19. The absolute SPL_p values are plotted at the proper frequency, f_p, determined for each noise source by use of equation (1). The haystack or SPL versus 1/3-octave band frequency plots shown in figure 20 then are used to construct the low-frequency noise source profiles beginning at the f_p-values (fig. 31(b)).

3. By use of the applicable equation (7), (8), or (9) determine the reduction in SPL at each frequency and plot the resulting spectrum together with steps 1 and 2 as shown in figure 31(c).

4. The complete spectrum for the configuration is then added antilogarithmically as shown in figure 31(d) by the solid curve. The dashed curve represents the original nozzle-only spectrum and is included for comparison.

5. The effect of forward velocity is now included by reducing the low frequency portion of the spectrum in figure 31(d) by use of the appropriate relative velocity; i.e., SPL - 10 log $(U_j - U_o)^n$. That part of the spectrum that represents the shielded jet noise is reduced by a function of 60 log $(U_j - U_o)$ as noted in reference 1. The resultant spectrum is shown in figure 31(e).

For full-scale CTOL-OTW configurations the low frequency jet-wing interaction noise may not be dominant over the jet noise. Also, attenuation of the low frequency noise sources could, perhaps, be achieved by use of surface treatments and trailing edge modifications that are beyond the scope of the present work. Consequently, step 2 may not necessary and one can proceed directly from step 1 to step 3. Once the static spectrum with jet noise shielding has been established, the effect of forward velocity reduces the entire spectrum by a function of 60 log $(U_j - U_o)$ as discussed in reference 1 and illustrated in figure 32. The latter procedure assumes that the low frequency is sufficiently below the configuration SPL with forward velocity that it does not represent a noise floor and becomes the dominant noise source.

CONCLUDING REMARKS

The results presented herein for a CTOL-OTW shielding experiment indicate that noise attenuation due to wing shielding takes place at the middle and high frequencies. At the low frequencies, however, there can be noise amplification due to the interaction of the jet exhaust flow and the wing.

E-7991

On the basis of the data presented herein, this low frequency noise amplification can be minimized by geometry considerations that include:

(1) Locating the nozzle significantly above the shielding surface.

(2) Large ratios of shielding surface length to nozzle exhaust diameter.

(3) Deflecting flaps downstream of the nozzle exhaust thereby minimizing scrubbing noise and increasing the distance between the exhaust jet and the trailing edge of the wing-flap system. Precise magnitudes for these geometry considerations depend on the specific application since the required aerodynamics and weight aspects for each CTOL-OTW application must be considered as well as the acoustic characteristics.

The present work has been limited to a conical nozzle and substantially unattached flow to the surface. It is interesting to note that attached flow acoustic data obtained with small-scale models reported in references 2 and 3 show low frequency noise sources similar to those noted for unattached flow. With attached flow; however, the jet noise shielding benefits appear to be less than those with unattached flow. Similar trends and observations were noted in unpublished NASA data in which a 10:1 slot nozzle was tested in a CTOL-OTW application.

While the acoustic correlation of jet noise shielding by a wing has been demonstrated herein for CTOL-OTW application, much further work remains to be done. So far the origin of the low frequency noise sources has not been identified, except in a gross manner. The relation of the jet velocity profiles to the OTW acoustics also has not been established. No explanation has been offered as to the low values of noise shielding achieved with CTOL-OTW configurations compared with the published barrier data. An explanation of this latter deficiency is of great interest for aircraft applications of the acoustic shielding concept since barrier theory indicates SPL shielding values of at least twice those reported herein.

NOMENCLATURE

(English units, except as noted)

a_o ambient speed of sound

B constant

D nozzle diameter

f 1/3 octave band spectrum frequency

f_b baseline frequency (eq. (1))

f_p peak frequency for given low frequency noise source

g constant, 32.2 ft/sec^2

h nozzle height above surface at exhaust plane

h_e effective nozzle height above surface at exhaust plane, $h + h_{te}/2$

h_{te} height from trailing edge to surface at nozzle exhaust plane, with or without flaps deflected

L shielding-surface length downstream of nozzle exhaust plane

L_f shielding-surface length upstream of nozzle exhaust plane

m,n variable exponents

Q,Z jet noise shielding correlation parameters

SPL sound pressure level of nozzle-surface configuration, dB re 2×10^{-5} N/m^2

SPL_N sound pressure level of nozzle only, dB

SPL_p peak sound pressure level, dB

SPL^* correlated peak sound pressure level, dB

ΔSPL $SPL - SPL_N$, dB

SPL_o local sound pressure level, dB

U_j jet velocity

U_o forward velocity

α board deflection angle

θ directivity angle

ρ_o ambient density

ϕ angle into shadow (barrier theory)

Subscripts:

I interaction noise source I

II interaction noise source II

E-7991

REFERENCES

1. von Glahn, U., Goodykoontz, J., and Wagner, J., "Nozzle Geometry and Forward Velocity Effects on Noise for CTOL Engine-Over-the-Wing Concept," TM X-71453, 1973, NASA.

2. Reshotko, M., Olsen, W. A., and Dorsch, R. G., "Preliminary Noise Tests of the Engine-Over-the-Wing Concept. 1: 30 Deg - 60 Deg Flap Position," TM X-68032, 1972, NASA.

3. Reshotko, M., Olsen, W. A., and Dorsch, R. G., "Preliminary Noise Tests of the Engine-Over-the-Wing Concept. 2: 10 Deg - 20 Deg Flap Position," TM X-68104, 1972, NASA.

4. Reshotko, M., Goodykoontz, J. H., and Dorsch, R. G., "Engine-Over-the-Wing Noise Research," TM X-68246, 1973, NASA.

5. McKinzie, D. J., Jr., and Burns, R. J., "Externally Blown Flap Trailing Edge Noise Reduction by Slot Blowing: A Preliminary Study," TM X-68172, 1973, NASA.

6. Kazin, S. B., and Pass, J. E., "NASA/GE Quiet Engine "C" Acoustic Test Results," CR-121176, 1974, NASA.

7. von Glahn, U., Groesbeck, D., and Goodykoontz, J., "Velocity Decay and Acoustic Characteristics of Various Nozzle Geometries with Forward Velocity," TM X-68259, 1973, NASA.

8. Richards, E., and Mead, D., Noise and Acoustic Fatigue in Aeronautics, John Wiley & Sons, Ltd., 1968, pp. 258-259.

9. Beranek, L. L., Noise Reduction, McGraw Hill Book Co., 1960, pp. 192-194.

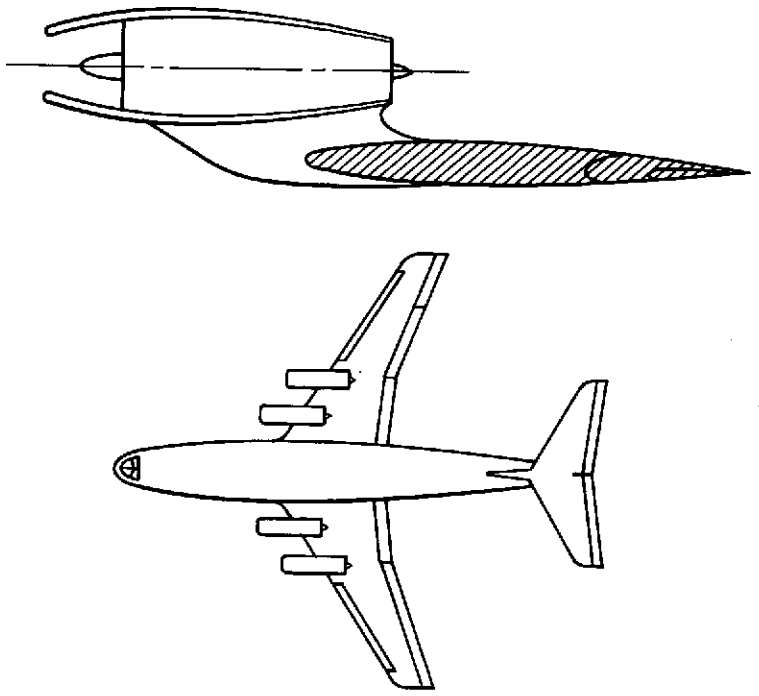

Figure 1. - Schematic of conventional (CTOL) airplane with engine over the wing (OTW).

E-7691

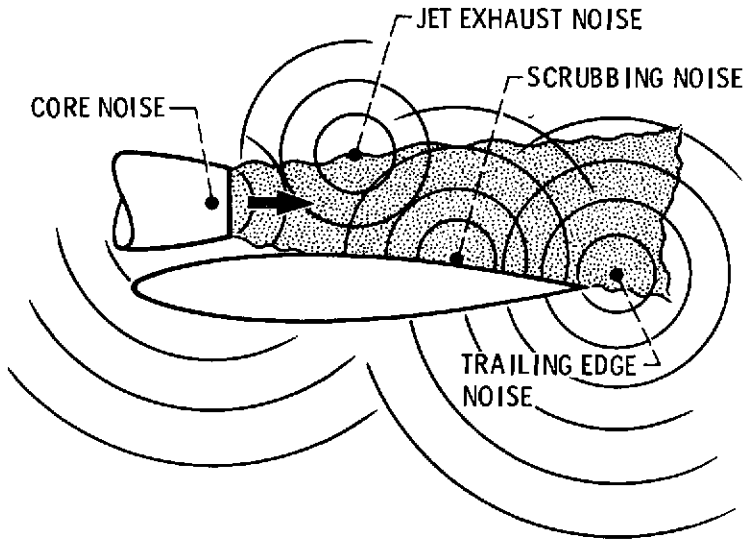

Figure 2. - CTOL-OTW configuration noise sources.

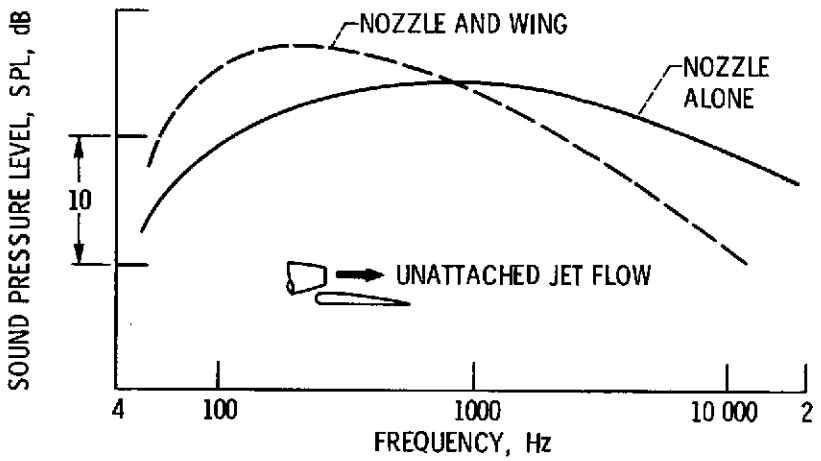

Figure 3. - Typical jet noise shielding with CTOL-OTW concept.

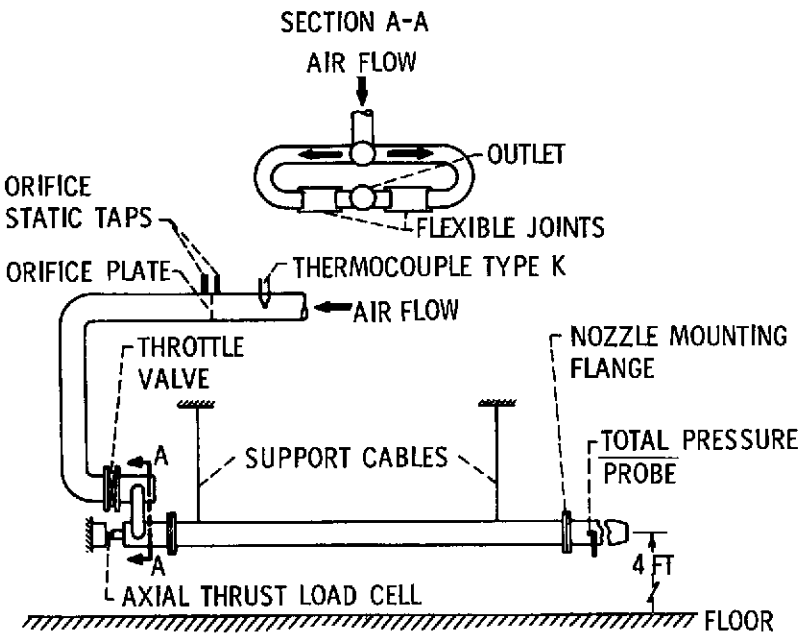

Figure 4. - Schematic diagram of courtyard test rig.

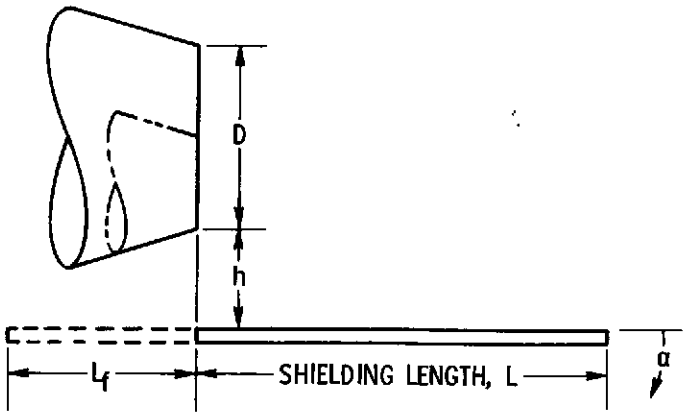

NOZZLE DIAMETER	L	L_f	SURFACE SPAN	NOMINAL NOZZLE HEIGHT, h	SHIELD DEFLECTION ANGLE, α, DEG
1.1, 2.1	5.9	2.6	24	0.57, 1.75, 3.0	0
	5.9	7.1	↓	↓	↓
	10.4	2.6			
	10.4	13.6			
	21.4	2.6	↓	↓	
1.1	10.4	13.6	96	0.57	↓
2.1	10.4	2.6	24	1.25	0.5, 10, 15

Figure 5. - Schematic sketch of courtyard rig CTOL-OTW test configuration. All dimensions in inches.

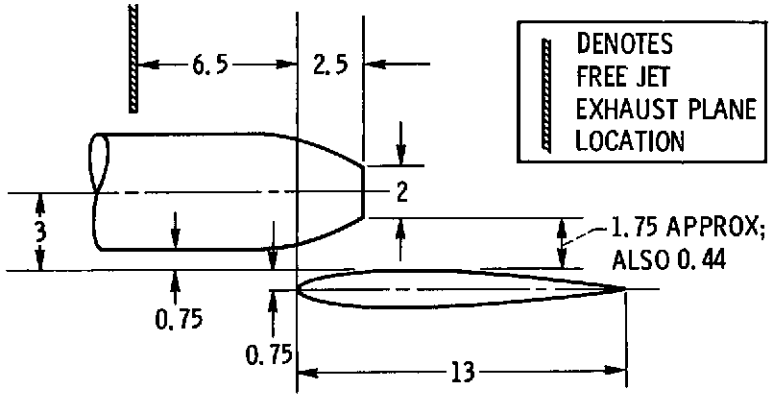

(a) CONVERGENT CIRCULAR NOZZLE.

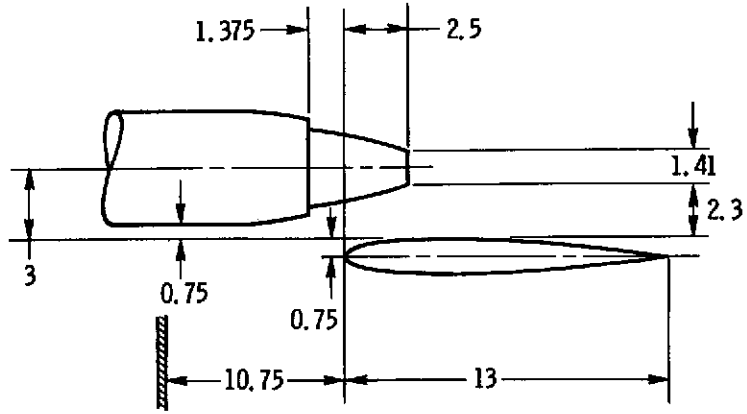

(b) BYPASS NOZZLE; CORE EXHAUST AT 20% CHORD.

Figure 6. - Small-scale CTOL-OTW configurations used for forward velocity studies (ref. 1). All dimensions in inches.

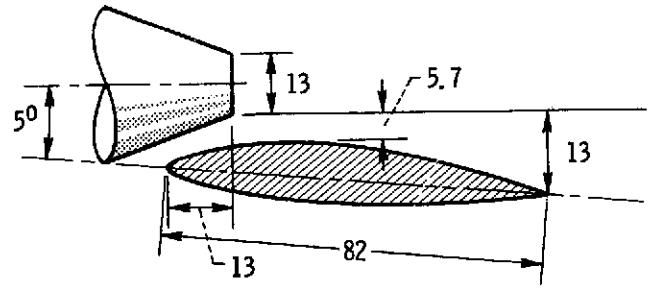

(a) ZERO FLAP DEFLECTION.

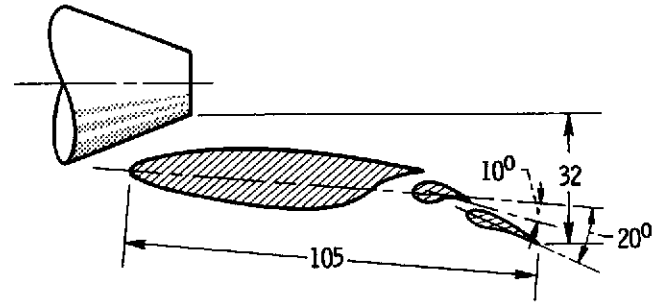

(b) 20° FLAP DEFLECTION.

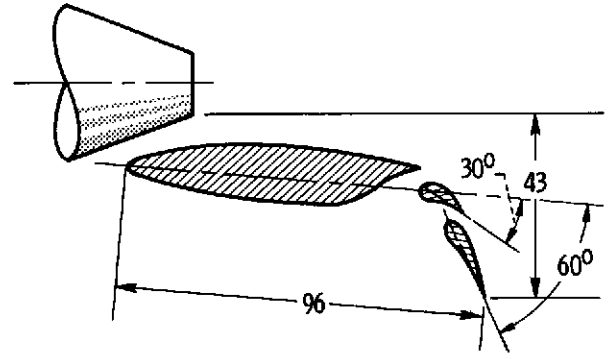

(c) 60° FLAP DEFLECTION.

Figure 7. - Large scale CTOL-OTW configuration from reference 4 cited in present work. All dimensions in inches.

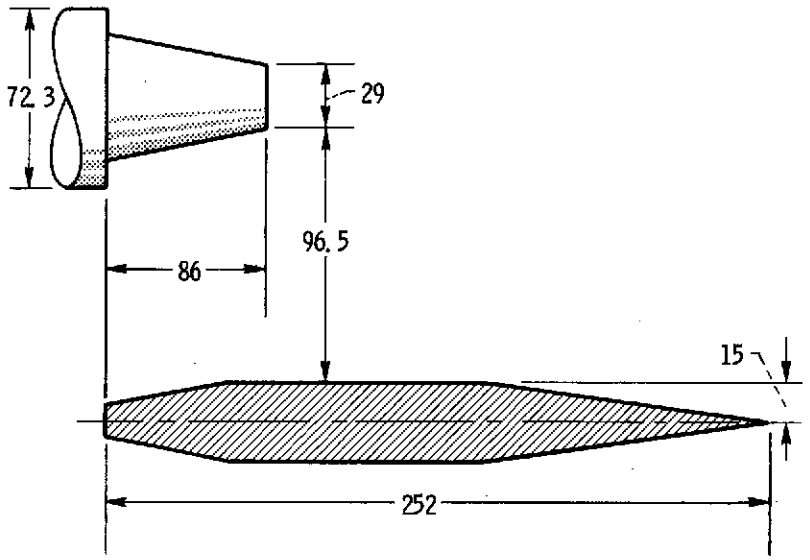

Figure 8. - Schematic sketch of quiet engine "C" in CTOL-OTW configuration. All dimensions in inches.

E-7991

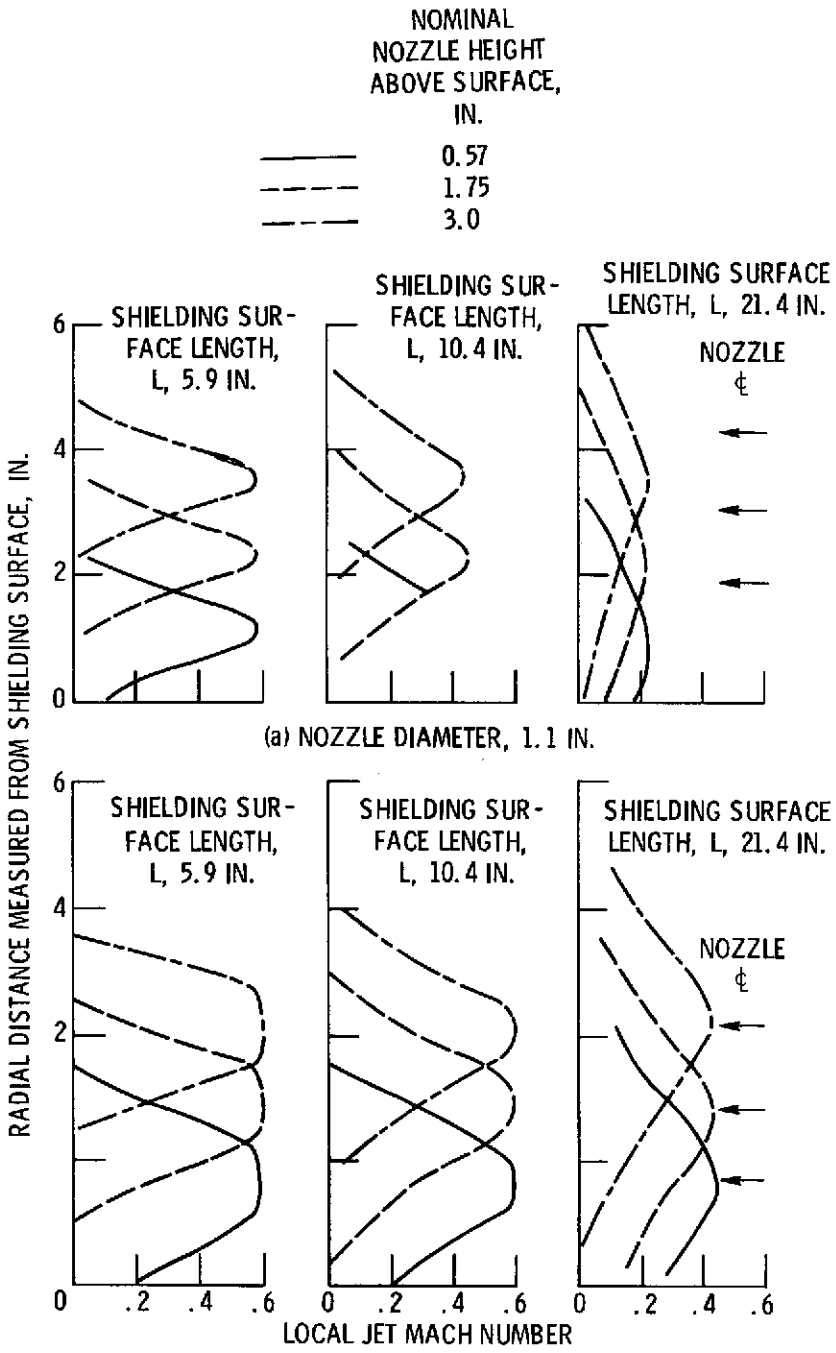

Figure 9. - Variation of velocity profile at shielding-surface trailing edge with nozzle-surface geometry. Jet velocity, 670 ft/sec.

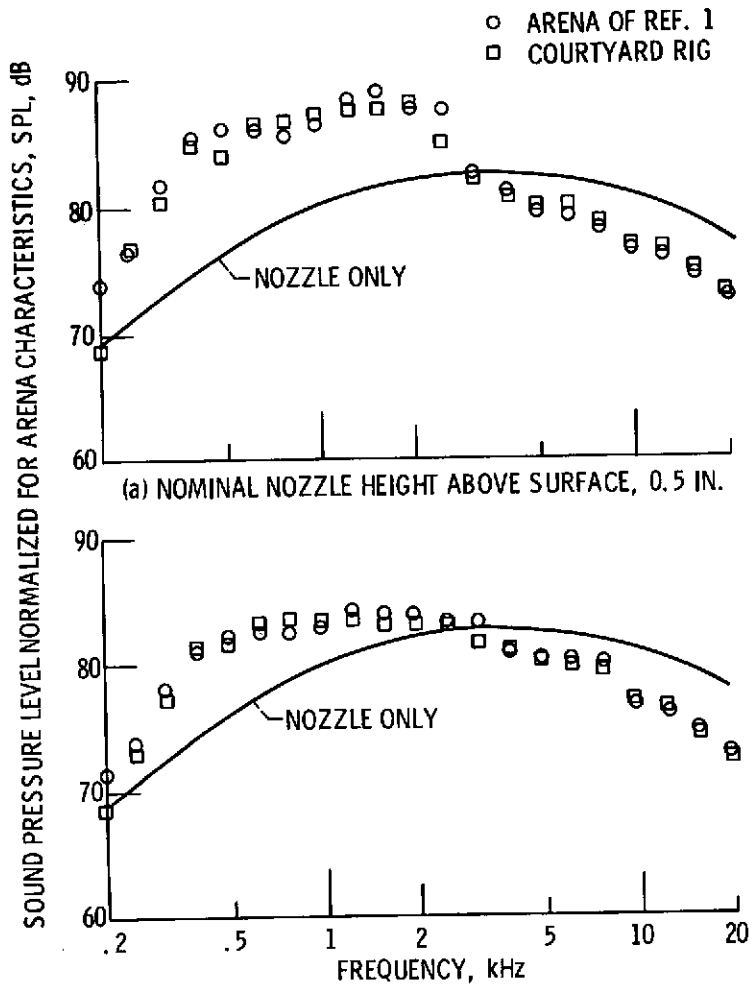

Figure 10. - Comparison of nozzle-wing noise characteristics in two acoustic arenas. Nominal nozzle diameter, 2 inches; wing chord, 13 inches; jet velocity, 840 ft/sec; directivity angle, 90^0; microphone radius, 10 feet.

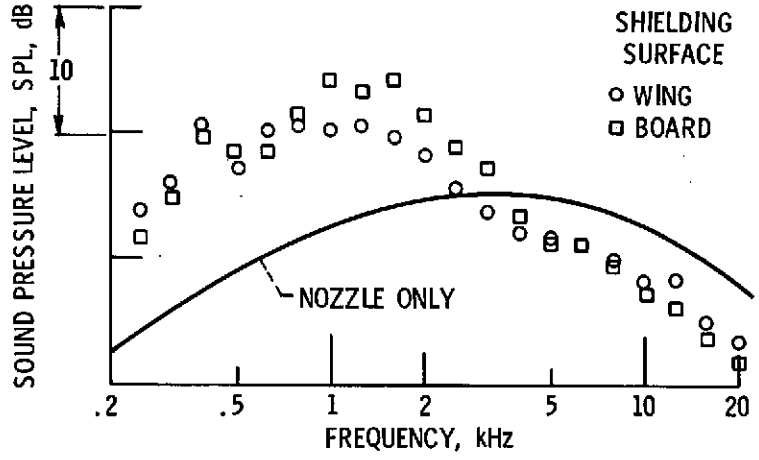

Figure 11. - Comparison of shielding characteristics for wing and board. Nozzle diameter, 2.1 inches; shielding surface length, L, 10.4 inches; nozzle height above surface, 0.57 inch; jet velocity, 670 ft/sec; directivity angle, 90^0.

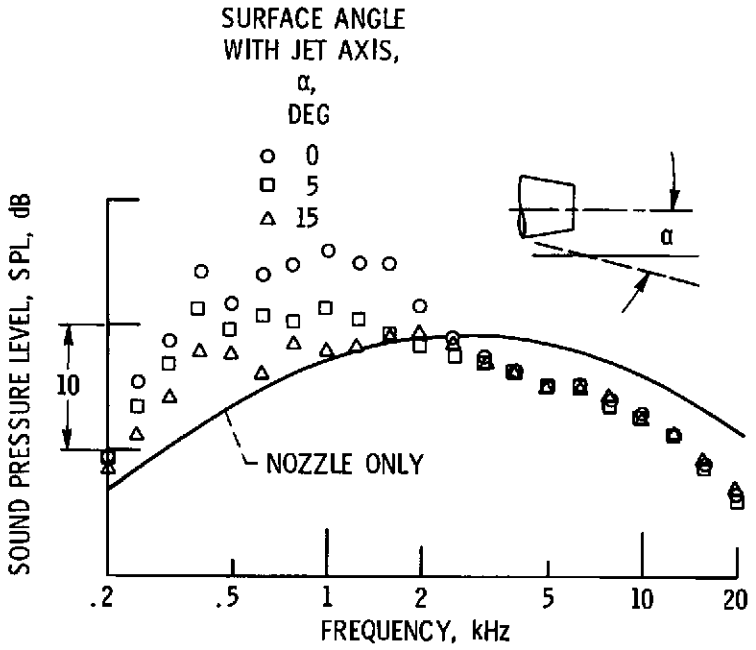

Figure 12. - Variation of sound pressure level with frequency for several board deflection angles. Nozzle diameter, 2.1 inches; shielding surface length, 10.4 inches; nozzle height above surface, 1.25 inches; jet velocity, 670 ft/sec; directivity angle, 90°.

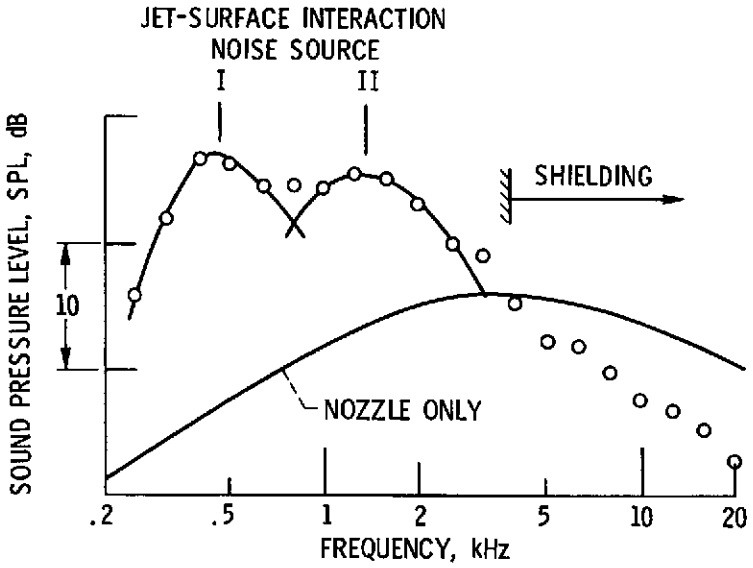

Figure 13. - Identification of low frequency noise sources. Noise diameter, 1.1 inches; shielding surface length, 10.4 inches; nozzle height above surface, 0.57 inch; jet velocity, 640 ft/sec; directivity angle, 90°.

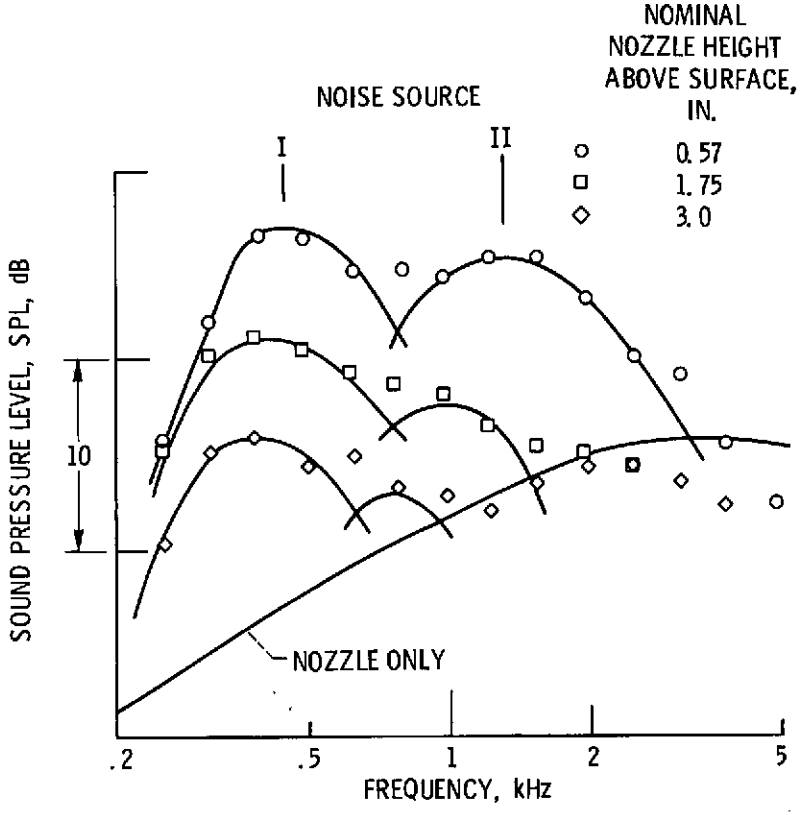

Figure 14. - Effect of nozzle height above shielding surface on low frequency jet-surface interaction noise sources. Nozzle diameter, 1.1 inches; shielding-surface length, 10.4 inches; jet velocity, 640 ft/sec; directivity angle, 90^0.

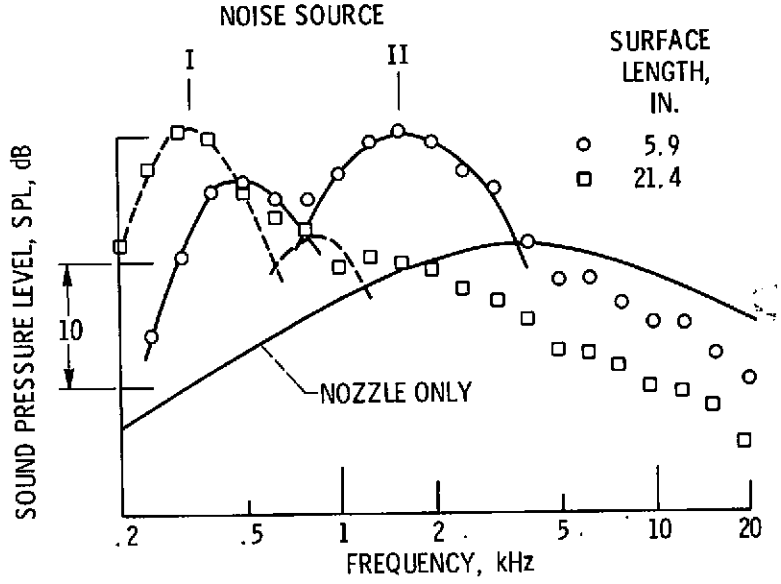

Figure 15. - Effect of shielding-surface length on low frequency jet-surface interaction noise sources. Nozzle diameter, 1.1 inches; nozzle height above shielding surface, 0.57 inch; jet velocity, 640 ft/sec; directivity angle, 90^0.

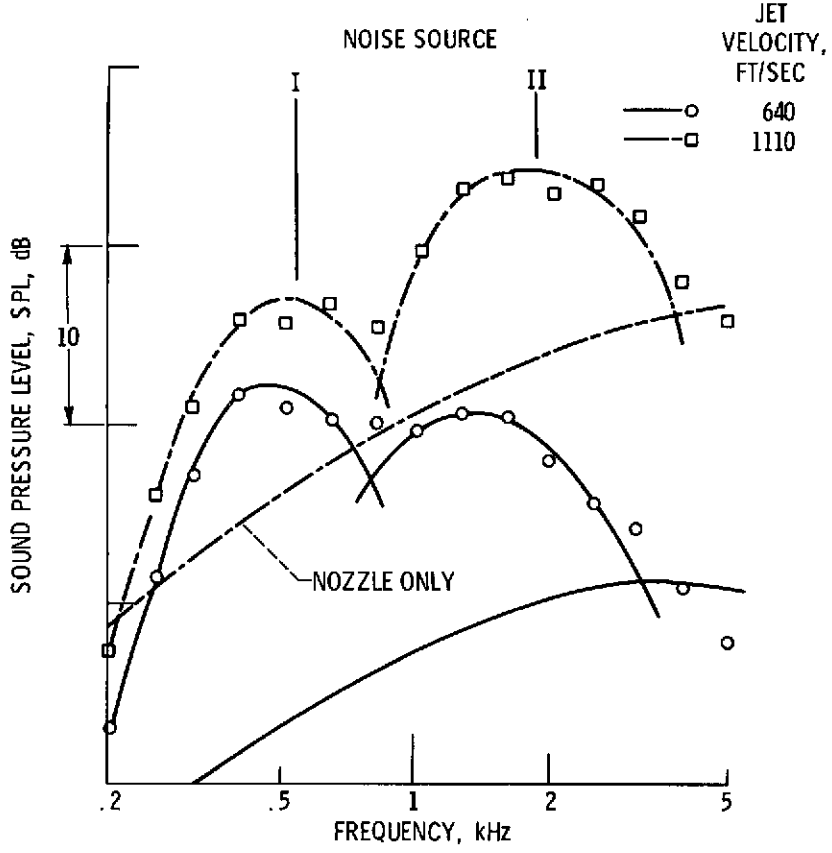

Figure 16. - Effect of jet velocity on low frequency jet-surface interaction noise sources. Nozzle diameter, 1.1 inches; shielding-surface length, 10.4 inches; nozzle height above surface, 0.57 inch.

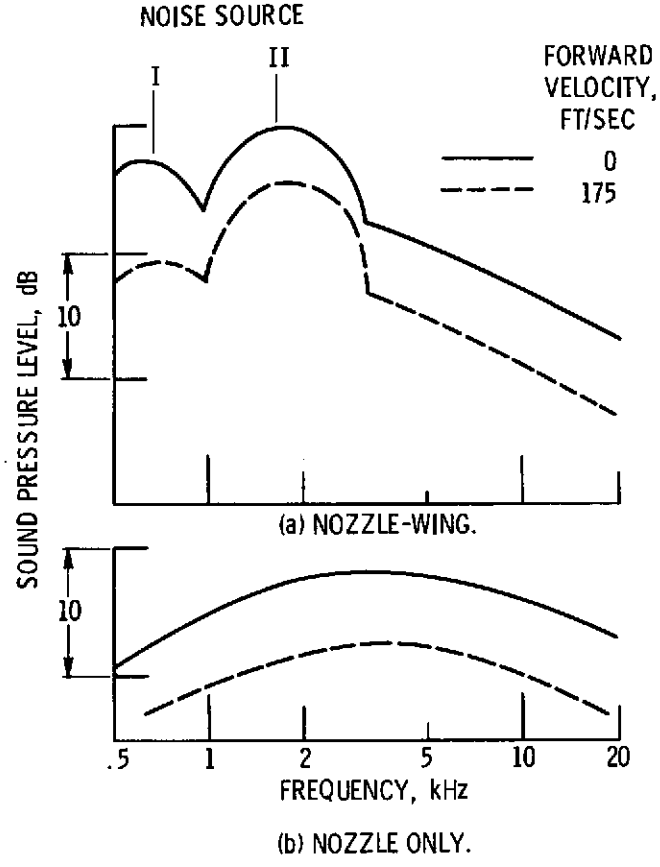

Figure 17. - Effect of forward velocity on jet-surface interaction noise sources. Nozzle diameter, 2 inches; nozzle height above surface, 0.44 inch; shielding-surface length, 10.4 inches; jet velocity, 840 ft/sec; directivity angle, 90^0.

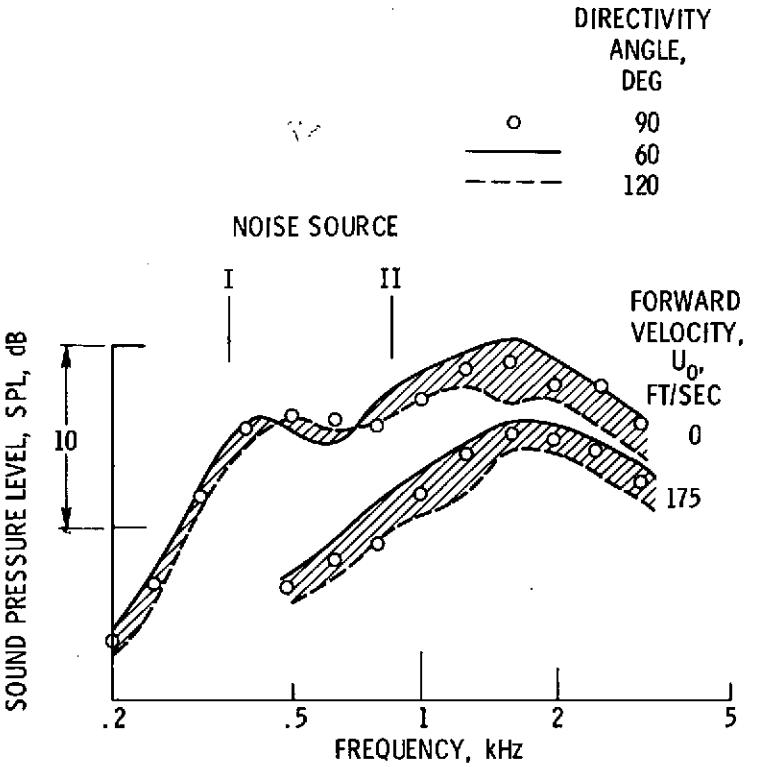

Figure 18. - Effect of directivity angle on jet-surface interaction noise sources. Nozzle diameter, 2 inches; nozzle height above surface, 0.44 inch; shielding-surface length, 10.4 inches; jet velocity, 840 ft/sec.

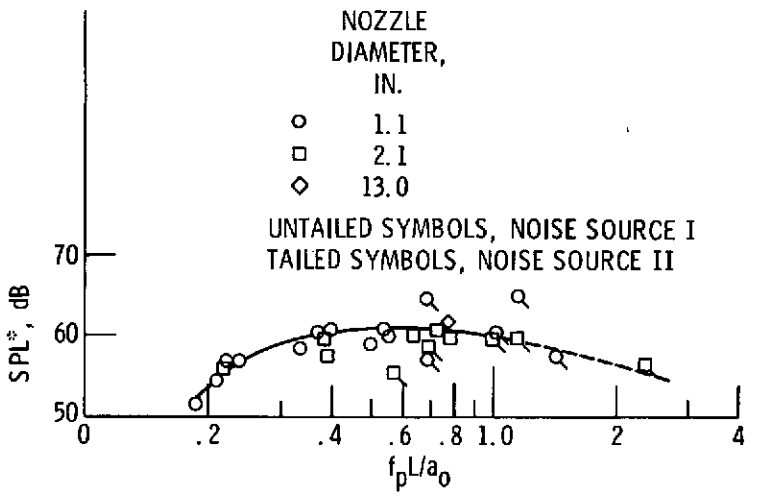

Figure 19. - Correlation of normalized peak sound pressure level for jet-surface interaction noise sources. Zero forward velocity. Microphone radius, 10 feet.

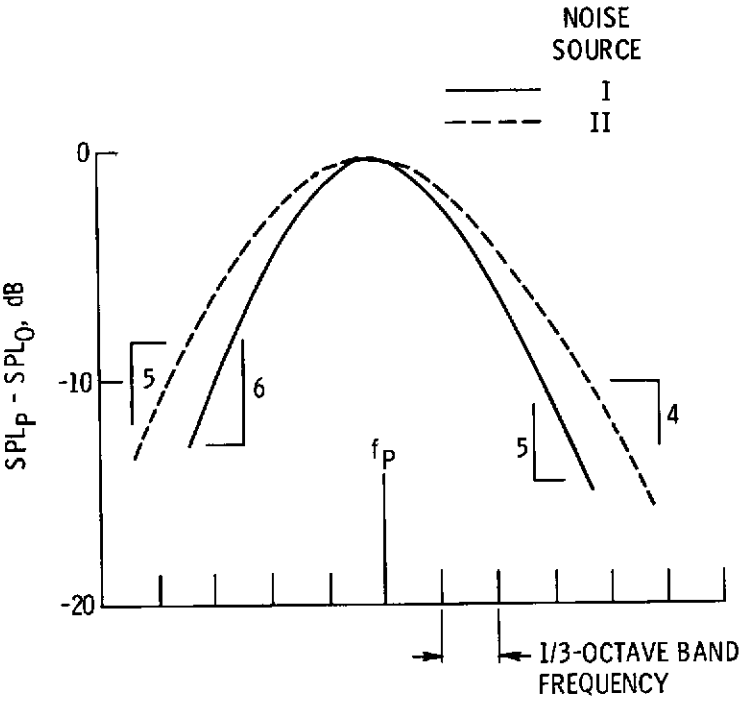

Figure 20. - Generalized jet-surface interaction noise source spectral distribution.

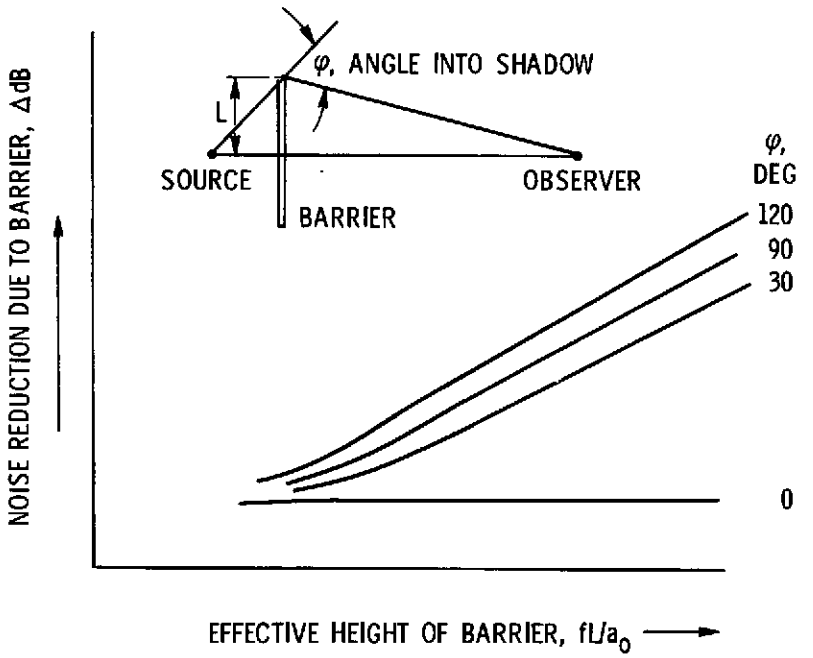

Figure 21. - Typical noise reduction due to barrier shielding (ref. 8).

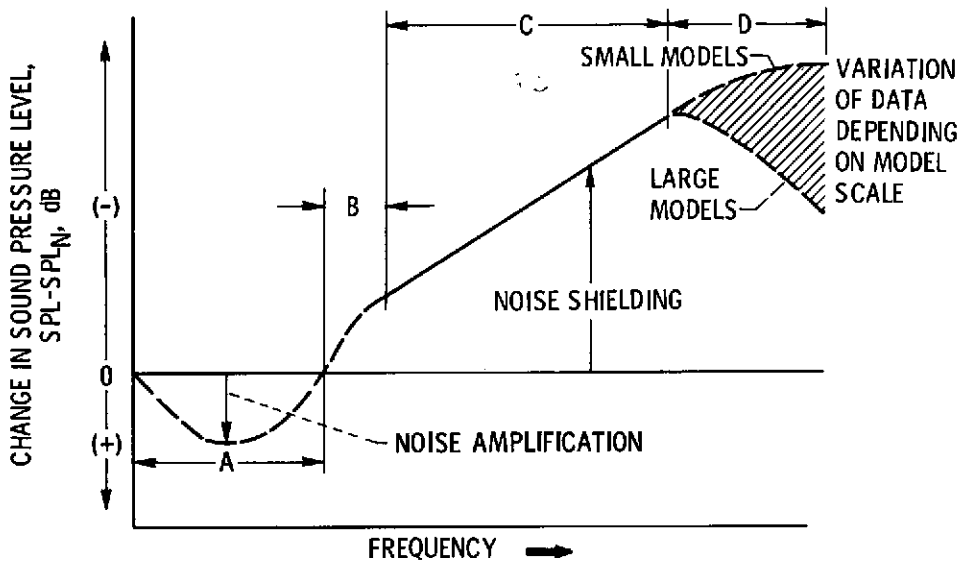

Figure 22. - Schematic representation of change in sound pressure level of jet noise due to a shielding surface.

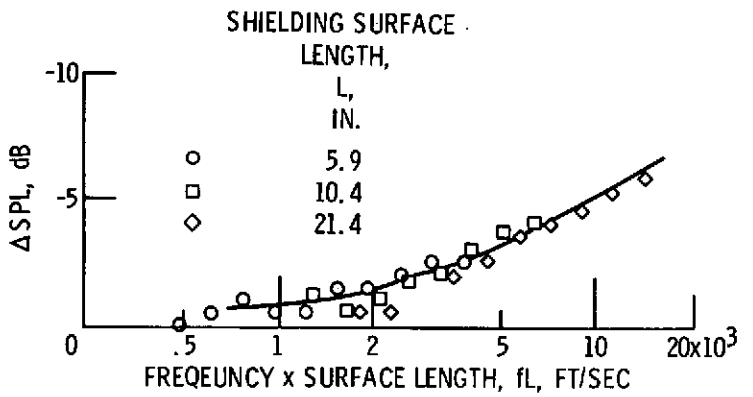

Figure 23. - Effect of surface length on jet noise shielding in region C. Nozzle diameter, 2.1 inches; nozzle height above surface, 3 inches; jet velocity, 670 ft/sec; directivity angle, 90^0.

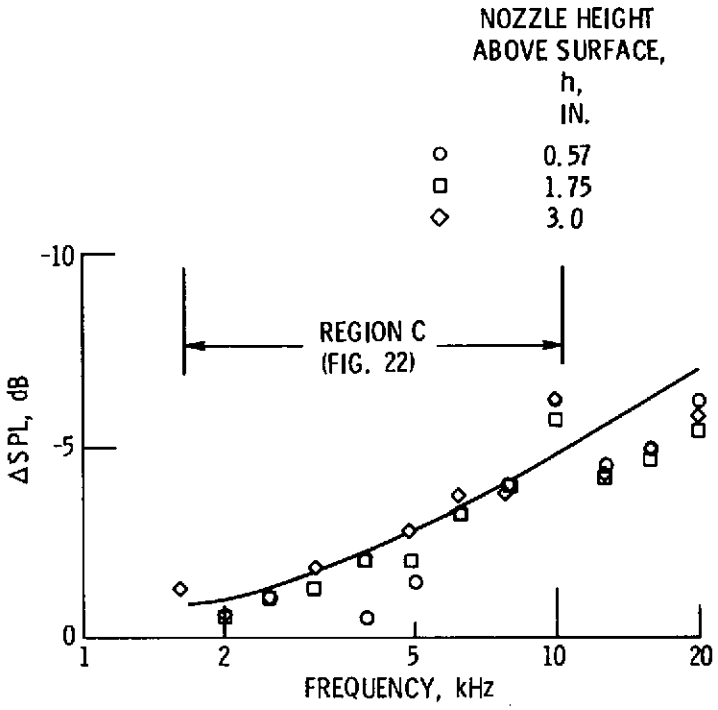

Figure 24. - Effect of nozzle height above surface on jet noise shielding. Nozzle diameter, 2.1 inches; shielding surface length, 10.4 inches; jet velocity, 670 ft/sec; directivity angle, 90^0.

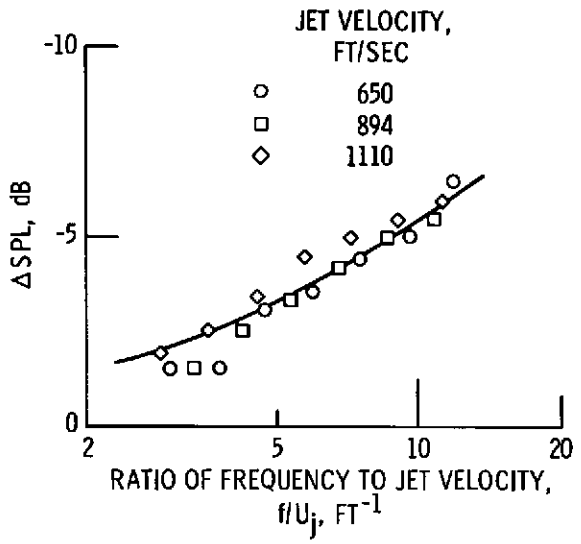

Figure 25. - Effect of jet velocity on jet noise shielding in region C. Nozzle diameter, 1.1 inches; nozzle height above surface, 3.0 inches; shielding-surface length, 10.4 inches; directivity angle, 90^0.

E-7991

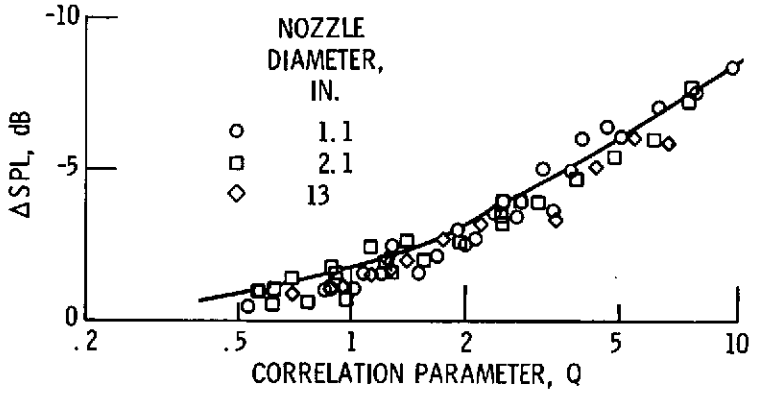

Figure 26. - Correlation of jet noise shielding including nozzle diameter effects, equation (5). Directivity angle, 90^0.

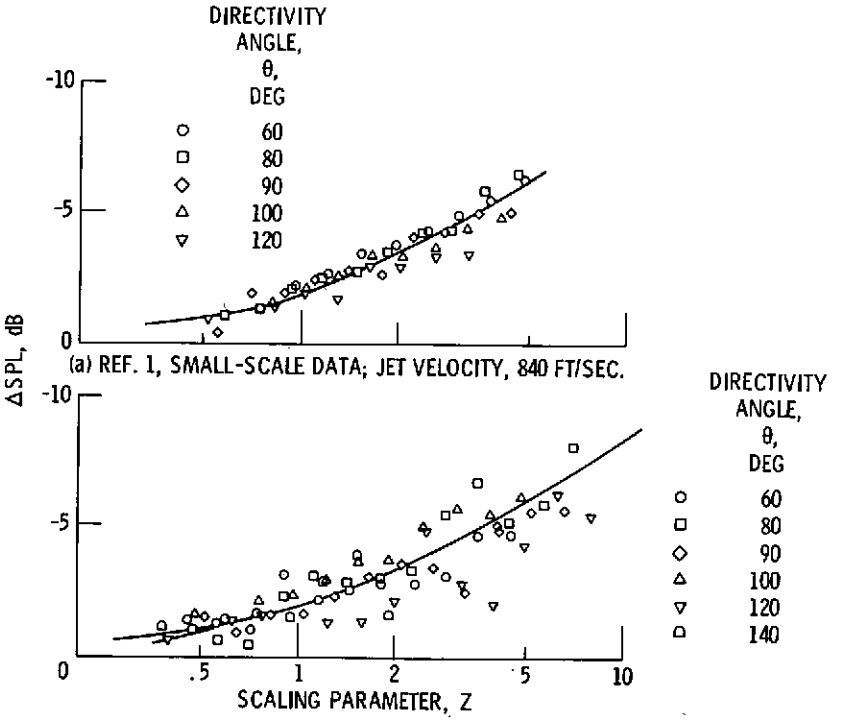

Figure 27. - Correlation of directivity angle effect on jet noise shielding.

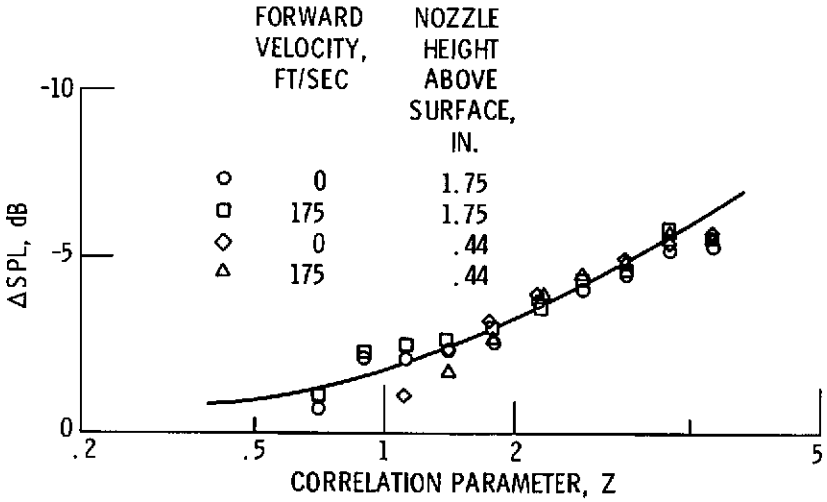

Figure 28. - Effect of forward velocity on correlation of jet-noise shielding. Directivity angle, 90^0; data from reference 1; jet velocity, 940 ft/sec; shielding-surface length, 10.4 inches; directivity angle, 90^0.

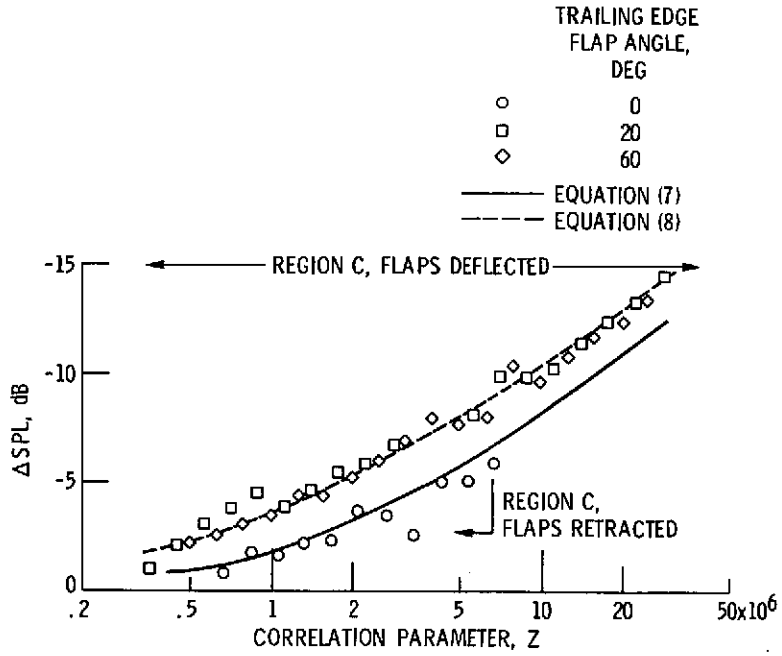

Figure 29. - Effect of flap deflection on jet noise shielding. Large-scale model (ref. 4); flap slots close; jet velocity, 675 ft/sec; directivity angle, 90^0.

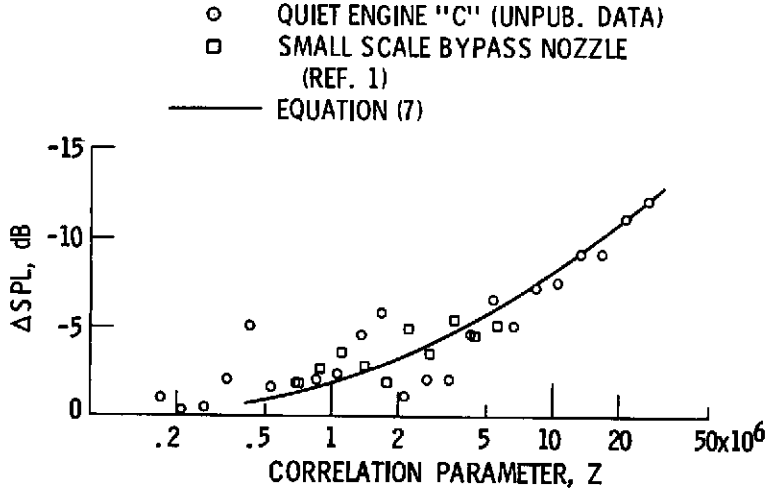

Figure 30. - Comparison of jet noise shielding with engine and small-scale model data. Bypass nozzle configurations. Directivity angle, 100°.

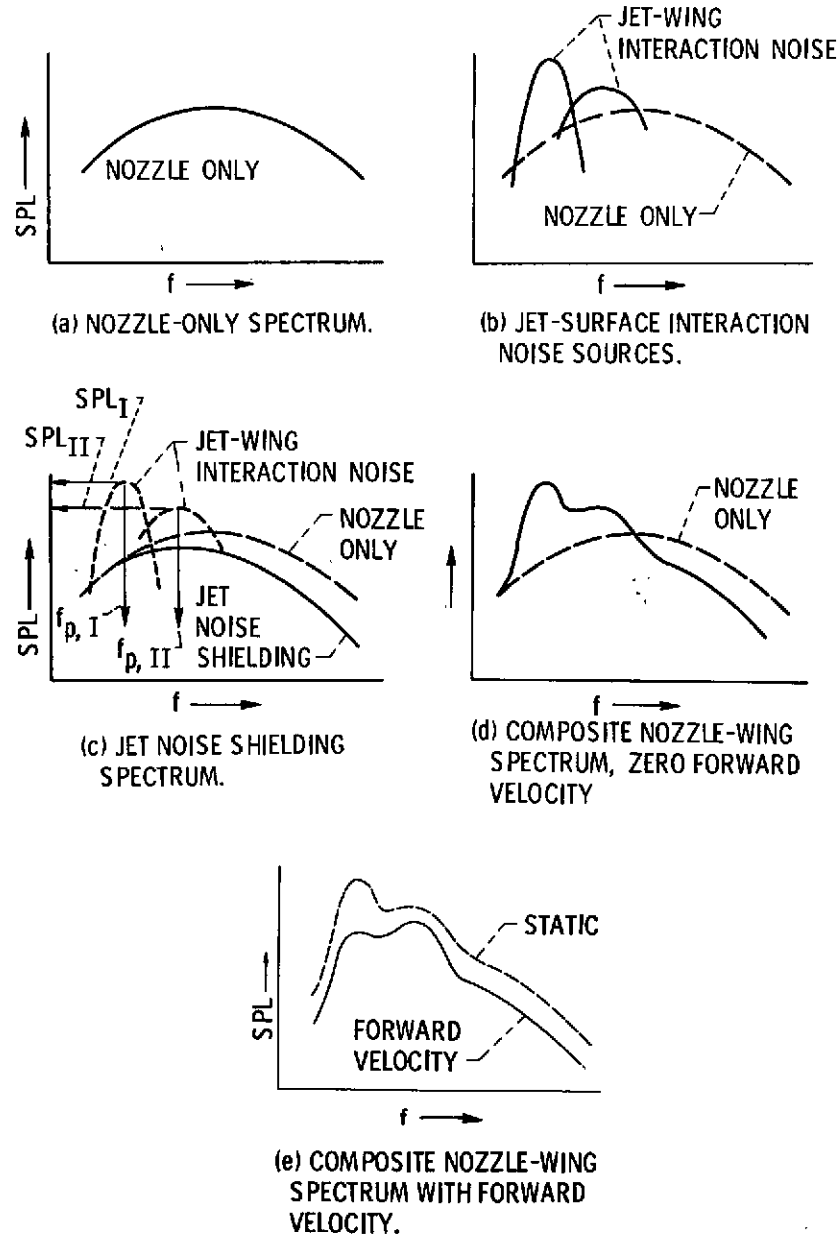

Figure 31. - Steps in the development of nozzle-wing noise spectrum prediction.

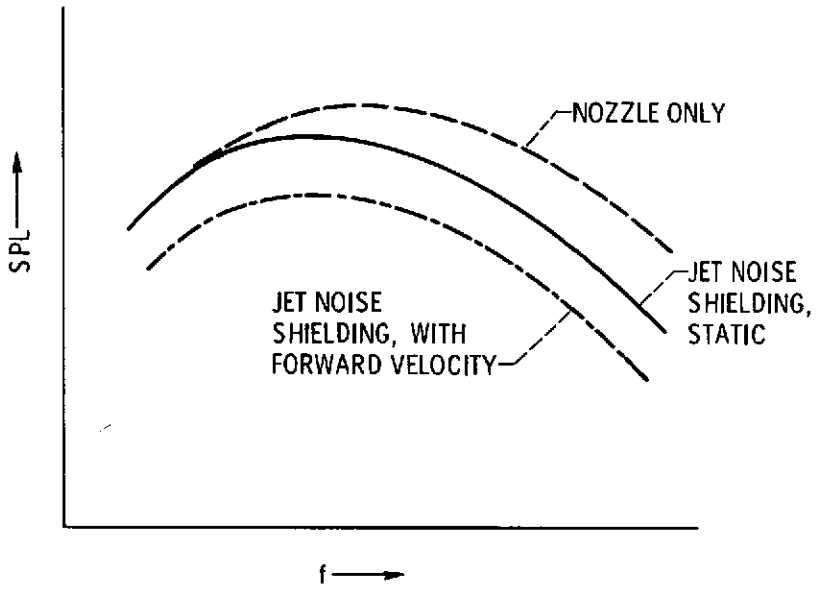

Figure 32. - Prediction technique development for nozzle-wing spectra without consideration of jet-surface interaction noise sources.